

# BARYON NUMBER TRANSFER IN HADRONIC INTERACTIONS

G. H. Arakelyan<sup>1</sup>, A. Capella, A. Kaidalov<sup>2</sup> and Yu. M. Shabelski<sup>3</sup>

Laboratoire de Physique Théorique\*,  
Université de Paris Sud, Bâtiment 210, 91405 Orsay Cedex, France  
E-mail: Alphonse.Capella@th.u-psud.fr

## ABSTRACT

The process of baryon number transfer due to string junction propagation in rapidity is considered. It has a significant effect in the net baryon production in  $pp$  collisions at mid-rapidities and an even larger effect in the forward hemisphere in the cases of  $\pi p$  and  $\gamma p$  interactions. The results of numerical calculations in the framework of the Quark-Gluon String model are in reasonable agreement with the data.

<sup>1</sup>Permanent address: Yerevan Physics Institute, Armenia and JINR, Dubna, Russia  
E-mail: argev@jerewan1.yerphi.am

<sup>2</sup>Permanent address: Institute of Theoretical and Experimental Physics, Moscow, Russia  
E-mail: kaidalov@vitep5.itep.ru

<sup>3</sup>Permanent address: Petersburg Nuclear Physics Institute, Gatchina, St.Petersburg, Russia  
E-mail: shabelsk@thd.pnpi.spb.ru

LPT-Orsay 01-24  
March 2001

---

\*Unité Mixte de Recherche - CNRS - UMR n° 8627

## 1. INTRODUCTION

The Quark–Gluon String Model (QGSM) and the Dual Parton Model (DPM) are based on the Dual Topological Unitarization (DTU) and describe quite reasonably many features of high energy production processes, including the inclusive spectra of different secondary hadrons, their multiplicities, KNO–distributions, etc., both in hadron–nucleon and hadron–nucleus collisions [1, 2, 3, 4]. High energy interactions are considered as proceeding via the exchange of one or several pomerons and all elastic and inelastic processes result from cutting through or between pomerons [5]. The possibility of exchanging a different number of pomerons introduces absorptive corrections to the cross sections which are in agreement with the experimental data on production of hadrons consisting of light quarks. Inclusive spectra of hadrons are related to the corresponding fragmentation functions of quarks and diquarks, which are constructed using the reggeon counting rules [6].

In the present paper we discuss the processes connected with the transfer of baryon charge over long rapidity distances. In the string models baryons are considered as configurations consisting of three strings attached to three valence quarks and connected in a point called “string junction” [7, 8]. Such a configuration corresponds in QCD to the following gauge-invariant operator

$$\psi_i(x_1)\psi_j(x_2)\psi_k(x_3)G[P(x_1, x)]_i^j G[P(x_2, x)]_j^k G[P(x_3, x)]_k^i \varepsilon^{i'j'k'} , \quad (1)$$

where

$$G[P(x_1, x)]_j^i = \left[ T \exp(g \int_{P(x_1, x)} A_\mu(x) dx^\mu) \right]_j^i . \quad (2)$$

It is very important to understand the role of the string-junction in the dynamics of high-energy hadronic interactions. Now we have several different experimental results concerning such processes. First of all the data [9] clearly show that in the forward hemisphere the number of secondary protons produced in  $\pi^+p$  interactions is significantly larger than the number of  $\bar{p}$  produced in  $\pi^-p$  collisions. This difference can not be described [4] without the assumption that the baryon charge is transferred from the target proton to the pion hemisphere.

Similar data on the differences of  $p - \bar{p}$  yields in  $\frac{1}{2}(\pi^+p + \pi^-p)$  collisions at 158 GeV/c were presented by the NA49 Coll. [10].

A second group of data concerns the energy dependence of the differences in yields of the protons and antiprotons at  $90^\circ$  (i.e. at  $x_F = 0$ ) at ISR energies [11].

Another sample of data includes the measurements of hyperon production asymmetries in 500 GeV/c  $\pi^-$ -nucleus interactions [12].

Finally, the proton-antiproton asymmetry in photoproduction was recently measured at HERA [13].

In this paper we present a simultaneous description of all these data and extract information on the properties of the string junction dynamics.

## 2. INCLUSIVE SPECTRA OF SECONDARY HADRONS IN QGSM

As mentioned above high energy hadron–nucleon and hadron–nucleus interactions are considered in the QGSM and in DPM as proceeding via the exchange of one or several pomerons. Each pomeron corresponds to a cylindrical diagram (see Fig. 1a), and thus, when cutting a pomeron two showers of secondaries are produced (Fig. 1b). The inclusive spectrum of secondaries is determined by the convolution of diquark, valence and sea quark distributions  $u(x, n)$  in the incident particles and the fragmentation functions  $G(z)$  of quarks and diquarks into secondary hadrons. The diquark and quark distribution functions depend on the number  $n$  of cut pomerons in the considered diagram. In the following we use the formalism of QGSM. In the case of a nucleon target the inclusive spectrum of a secondary hadron  $h$  has the form [1]:

$$\frac{x}{\sigma_{inel}} \frac{d\sigma}{dx} = \sum_{n=1}^{\infty} w_n \phi_n^h(x) \quad , \quad (3)$$

where the functions  $\phi_n^h(x)$  determine the contribution of diagrams with  $n$  cut pomerons and  $w_n$  is the probability of this process. Here we neglect the contributions of diffraction dissociation processes which are comparatively small in most of the processes considered below. It can be accounted for separately [1, 2, 4].

For  $pp$  collisions

$$\phi_{pp}^h(x) = f_{qq}^h(x_+, n) f_q^h(x_-, n) + f_q^h(x_+, n) f_{qq}^h(x_-, n) + 2(n-1) f_s^h(x_+, n) f_s^h(x_-, n) \quad , \quad (4)$$

$$x_{\pm} = \frac{1}{2} [\sqrt{4m_T^2/s + x^2} \pm x] \quad , \quad (5)$$

where  $f_{qq}$ ,  $f_q$  and  $f_s$  correspond to the contributions of diquarks, valence and sea quarks respectively. They are determined by the convolution of the diquark and quark distributions with the fragmentation functions, e.g.,

$$f_q^h(x_+, n) = \int_{x_+}^1 u_q(x_1, n) G_q^h(x_+/x_1) dx_1 \quad . \quad (6)$$

In the case of a meson beam the diquark contributions in Eq. (4) should be changed by the contribution of valence antiquarks:

$$\phi_{\pi p}^h(x) = f_q^h(x_+, n) f_q^h(x_-, n) + f_q^h(x_+, n) f_{qq}^h(x_-, n) + 2(n-1) f_s^h(x_+, n) f_s^h(x_-, n) \quad . \quad (7)$$

The diquark and quark distributions as well as the fragmentation functions are determined from Regge intercepts. Their expressions are given in Appendix 1.

The net baryon charge can be obtained from the fragmentation of the diquark giving rise to a leading baryon (Fig. 2a). A second possibility is to produce a (leading) meson in the first break-up of the string and the baryon in a subsequent break-up (Fig. 2b).

As discussed above, in the approach [7, 8] the baryon consists of three valence quarks together with string junction (SJ), which is conserved during the interaction<sup>†</sup>.

This gives a third possibility for secondary net baryon production in non-diffractive hadron-nucleon interactions (Fig. 2c).

The secondary baryon consists of the SJ together with two valence and one sea quarks (Fig. 2a), one valence and two sea quarks (Fig. 2b) or three sea quarks (Fig. 2c). The fraction of the incident baryon energy carried by the secondary baryon decreases from a) to c), whereas the mean rapidity gap between the incident and secondary baryon increases.

The probability to find a comparatively slow SJ in the case of Fig. 2c can be estimated from the data on  $\bar{p}p$  annihilation into mesons (see Figs. 1c, d). This probability is known experimentally only at comparatively small energies where it is proportional to  $s^{\alpha_{SJ}-1}$  with  $\alpha_{SJ} \sim 0.5$ .

However, it has been argued [14] that the annihilation cross section contains a small piece which is independent of  $s$  and thus  $\alpha_{SJ} \sim 1$ . Irrespectively of the value of  $\alpha_{SJ}$ , the contribution of the graph in Fig. 2c corresponds to annihilation and, thus, has a small coefficient which will be denoted by  $\varepsilon$ . In our calculation we shall use

$$\alpha_{SJ} = 0.5 \tag{8}$$

and will treat  $\varepsilon$  as a free parameter. A contribution with  $\alpha_{SJ} \sim 1$ , if present at all, is expected to be important only at very high energies (see a discussion of this point in section 5). The values of  $\alpha_{SJ}$  and  $\varepsilon$  can only be determined with the help of accurate data.

### 3. COMPARISON WITH THE DATA

The mechanism of the baryon charge transfer via SJ without valence quarks (Fig. 2c) was not accounted for in previous papers [1, 2, 3, 4].

The data at comparatively low energies ( $\sqrt{s} \sim 15 \div 40$  GeV) can be described with  $\alpha_{SJ} = 0.5$ . Unfortunately, the value of  $\varepsilon$  cannot be determined in a unique way. Many sets of data can be described with  $\varepsilon = 0.05$ . However, other data sets favor a value four times larger,  $\varepsilon = 0.2$ . Because of that, we will present our results for these two values of  $\varepsilon$ , leaving all other parameters in the model unchanged. Thus, the results for meson and antibaryon production are the same in the two cases.

The inclusive spectra of secondary protons and antiprotons produced in  $pp$  collisions at lab. energies 100 and 175 GeV [9] are shown in Figs. 3a and 3b together with the curves calculated in the QGSM. The agreement of our results with  $\varepsilon = 0.05$  with the data is quite reasonable, on the same level (or even better) as in the previous papers which

---

<sup>†</sup>At very high energies one or even several SJ pairs can be produced.

did not incorporate the SJ mechanism of Fig. 2c. The variant with  $\varepsilon = 0.2$  gives too large multiplicity of secondary protons at small  $x_F$ . The description of the antiproton yields is reasonable.

The data of Ref. [15] are in some regions of  $x_F$  in disagreement with the data of Ref. [9] as well as with our calculations. However, one can see from Figs. 3c and 3d that the experimental points can not be described by any smooth curve. Probably this is connected with the use of different detectors for different  $x_F$  regions and to the influence of the trigger in [15]. Again, the value  $\varepsilon = 0.05$  is preferable.

The data on secondary proton and antiproton production in  $pp$  collisions at ISR energies [11] at  $90^\circ$  in c.m.s. are presented in Figs. 3e and 3f. Their differences, which are more sensitive to the baryon charge transfer, are presented in Fig. 3g. One can see that the last data, as well as the yields of protons and antiprotons separately, are described quite reasonably by QGSM with  $\varepsilon = 0.2$ . However, it is necessary to note, that the systematic errors in [11] are of the order of 30 %, so the value  $\varepsilon = 0.05$  can not be excluded. Thus the disagreement between ISR data [11] and more recent data [9, 15] on spectra of protons in  $pp$ -collisions does not allow to determine uniquely the value of  $\varepsilon$ .

The data on baryon production in the pion fragmentation region [9] are presented in Fig. 4. The spectra of antiprotons produced in  $\pi^-p$  collisions, shown in Fig. 4a, allows one to fix the fragmentation function of a quark into baryon/antibaryon. If the contribution of the baryon charge transfer were negligibly small, the inclusive spectra of reactions  $\pi^-p \rightarrow \bar{p}X$  and  $\pi^+p \rightarrow pX$  in the pion fragmentation region would be practically the same [4]. Actually, the data for the second reaction are significantly higher than for the first one providing evidence for the baryon charge transfer due to the SJ propagation. The difference of the inclusive spectra in the two considered processes allows one to estimate quantitatively the contribution of the baryon charge transfer, and the parametrization of these processes given in Appendix leads to a reasonable description of proton yields in  $\pi^+p$  collisions with  $\varepsilon = 0.2$ . The value  $\varepsilon = 0.05$  seems to be too small here. Note, however, that our factorized formulae, Eqs. 4 and 7, imply that the slowed down proton is made out of SJ and three sea quarks (see Fig. 2c). Thus, they should be modified for the reaction  $\pi^+p \rightarrow pX$  in the pion fragmentation region due to the possibility of SJ recombination with a pion valence quark – which would change the ratio of protons and neutrons. A simple estimate based on the quark combinatorics given in Appendix 1 leads to an increase of the proton yield in the reaction  $\pi^+p \rightarrow pX$  by about 50 %. In this case the value of  $\varepsilon = 0.05$  can be consistent with the data. This problem disappears if we consider the sum of  $\pi^+p$  and  $\pi^-p$ . Preliminary data on  $\frac{1}{2}(\pi^+p + \pi^-p) \rightarrow (p - \bar{p})X$  were obtained by the NA49 Coll. [10]. One can see from Fig.4c, that they are in good agreement with our calculations with  $\varepsilon = 0.05$  and in total disagreement with  $\varepsilon = 0.2$ .

The data on  $\Lambda$  and  $\bar{\Lambda}$  production in  $pp$  collisions [16, 17, 18, 19], presented in Fig. 5, are also in agreement with QGSM and the value  $\varepsilon = 0.05$  is again favored.

In Fig. 6 we show the data [12] on the asymmetry of strange baryons produced in  $\pi^-$  interactions<sup>‡</sup> at 500 GeV/c. The asymmetry is determined as

$$A(B/\bar{B}) = \frac{N_B - N_{\bar{B}}}{N_B + N_{\bar{B}}} \quad (9)$$

for each  $x_F$  bin.

The theoretical curves for the data on all asymmetries calculated with  $\varepsilon = 0.05$  are in reasonable agreement with the data with the exception of  $\Xi^-/\Xi^+$  at positive  $x_F$ . However in this region the effect of recombination of SJ with valence (d) quark of  $\pi^-$  can be important and can lead to an increase of cross section analogous to the one in  $\pi^+p \rightarrow pX$  discussed above. In the case of  $\Omega/\bar{\Omega}$  production we predict a non-zero asymmetry in agreement with experimental data. Let us note that the last asymmetry is absent, say, in the naive quark model because  $\Omega$  and  $\bar{\Omega}$  have no common valence quarks with the incident particles. The value  $\varepsilon = 0.2$  seems to be excluded.

Preliminary data on  $p/\bar{p}$  asymmetry in  $ep$  collisions at HERA were presented by the H1 Collaboration [13]. Here the asymmetry is defined as

$$A_B = 2 \frac{N_p - N_{\bar{p}}}{N_p + N_{\bar{p}}}, \quad (10)$$

i.e. with an additional factor 2 in comparison with Eq. (9). The experimental value of  $A_B$  is equal to  $8.0 \pm 1.0 \pm 2.5$  % [13] for secondary baryons produced at  $x_F \sim 0.04$  in the  $\gamma p$  c.m. frame. QGSM with  $\varepsilon = 0.05$  predicts here 2.9 %, i.e. a smaller value, whereas the calculation with  $\varepsilon = 0.2$  gives the value 7.7 %, in agreement with the data.

## 5. CONCLUSIONS

We have demonstrated that experimental data on high-energy hadronic interactions support the possibility of baryon charge transfer over large rapidity distances. Probably, the most important are the baryon-antibaryon asymmetry in  $\Omega$  and  $\bar{\Omega}$  [12] in  $\pi^-p$  collisions, where both secondary particles have no common valence quarks with the incident particles. This asymmetry is provided by baryon charge transfer due to string junction diffusion.

Also the production of net baryons in  $\pi p$  and  $\gamma p$  interactions in the projectile hemisphere provides good evidence for such a mechanism.

As for the values of the parameters  $\alpha_{SJ}$  and  $\varepsilon$  which govern the baryon charge transfer we have seen that the data, at comparative low energies ( $\sqrt{s} \sim 15 \div 40$  GeV), without providing a clear cut answer, strongly favor the values  $\alpha_{SJ} = 0.5$  and  $\varepsilon = 0.05$ . Indeed,

---

<sup>‡</sup>These data were obtained from pion interactions on a nuclear target where different materials were used in a very complicated geometry. We assume that the nuclear effects are small in the asymmetry ratio (9), and compare the pion-nucleus data with calculations for  $\pi^-p$  collisions.

as discussed above, the data which favor  $\varepsilon = 0.2$  have either a large systematic error [11] or correspond to situations where effects, not incorporated in the present version of the model, are expected to be important (as in  $\pi^+p \rightarrow pX$  ; see the discussion in Section 3).

At HERA energies the situation is different. Here the observed asymmetry is better described with  $\varepsilon = 0.2$ . Note, however, that HERA data are preliminary and have rather large errors (the prediction for asymmetry with  $\varepsilon = 0.05$  deviates from the data by about two standard deviations). If this discrepancy is real can it be solved ? The data at  $\sqrt{s} \lesssim 40$  GeV that we have examined provide information for the transfer of baryon charge over about five rapidity units. In contrast, the HERA data provide information for the corresponding transfer over more than seven units. In ref. [21] HERA data were described under the assumption that there is a component with  $\alpha_{SJ} \approx 1$  and a very small strength. Another possibility would be to use  $\alpha_{SJ} \simeq 0.5$  and to assume, following Ref. [22]-[24] that the strength of the  $SJ$  transfer contribution increases with the number of inelastic collisions. In this way the asymmetry would increase with energy since the average number of inelastic collisions, determined from Eqs. (42) and (43), increases with  $s$ . (This mechanism also allows to explain the increase of stopping in heavy ion collisions with increasing centrality) [22]-[26].

In conclusion, the study of the transfer of baryon charge over large rapidity distances is very important. Good experimental data in  $pp$ ,  $pA$  and  $AB$  collisions for different centralities are needed in order to understand the dynamics of this mechanism.

Acknowledgments: We thank H.G.Fisher from NA49 Collaboratiomn for providing the preliminary data in Fig. 4c prior to publication.

This paper was supported by grant NATO OTR. LG 971390 and NATO PSTCLG 977275.

## APPENDIX. QUARK AND DIQUARK DISTRIBUTIONS AND THEIR FRAGMENTATION FUNCTIONS

In the present calculations we use quark and diquark distributions in the proton for one-pomeron exchange given by the correspondent Regge behaviour [1]

$$u_{uu}(x, n) = C_{uu}x^{\alpha_R-2\alpha_B+1}(1-x)^{-\alpha_R}, \quad (11)$$

$$u_{ud}(x, n) = C_{ud}x^{\alpha_R-2\alpha_B}(1-x)^{-\alpha_R}, \quad (12)$$

$$u_u(x, n) = C_u x^{-\alpha_R}(1-x)^{\alpha_R-2\alpha_B+1}, \quad (13)$$

$$u_d(x, n) = C_d x^{-\alpha_R}(1-x)^{n+\alpha_R-2\alpha_B}, \quad (14)$$

$$(15)$$

In the case of multipomeron exchange the distributions of valence quarks and diquarks are softened due to the appearance of sea quark contribution. Also it is necessary to

account that  $d$ -quark distribution is more soft in comparison with  $u$ -quark one. There is some freedom [3] how to account for these effects. We use the simplest way and write diquark and quark distributions (for  $\alpha_R = 0.5$  and  $\alpha_B = -0.5$ ) as

$$u_{uu}(x, n) = C_{uu}x^{\alpha_R-2\alpha_B+1}(1-x)^{frac{43(n-1)-\alpha_R}, \quad (16)$$

$$u_{ud}(x, n) = C_{ud}x^{\alpha_R-2\alpha_B}(1-x)^{n-1-\alpha_R}, \quad (17)$$

$$u_u(x, n) = C_u x^{-\alpha_R}(1-x)^{n+\alpha_R-2\alpha_B+1}, \quad (19)$$

$$u_d(x, n) = C_d x^{-\alpha_R}(1-x)^{\frac{4}{3}(n-1)+\alpha_R-2\alpha_B+1}, \quad (21)$$

$$u_{\bar{u}}(x, n) = u_{\bar{d}}(x, n) = C_{\bar{u}}x^{-\alpha_R} \times [(1-x)^{n+\alpha_R-2\alpha_B-1} - \delta/2(1-x)^{n+2\alpha_R-2\alpha_B-1}], n > 1, \quad (23)$$

$$u_s(x, n) = C_s x^{-\alpha_R}(1-x)^{n+2\alpha_R-2\alpha_B-1}, n > 1. \quad (24)$$

In the case of a pion beam we use

$$u_q(x, n) = C_q x^{-\alpha_R}(1-x)^{n-\alpha_R-1}, u_{\bar{q}}(x, n) = C_{\bar{q}} x^{-\alpha_R}(1-x)^{n-\alpha_R-1}, \quad (25)$$

for valence quarks, and

$$u(x, n) = Cx^{-\alpha_R}(1-x)^{n-\alpha_R-1}[1 - \delta\sqrt{1-x}], n > 1, \quad (26)$$

$$u_s(x, n) = C_s x^{-\alpha_R}(1-x)^{n-1}, n > 1, \quad (26)$$

for sea quarks, where  $\delta = 0.2$  is the relative probability to find a strange quark in the sea. The values of  $\alpha_R$  and  $\alpha_B$  are given in Table 1. The factors  $C_i$  are determined from the normalization condition

$$\int_0^1 u_i(x, n)dx = 1. \quad (27)$$

and sum rule

$$\int_0^1 \sum_i u_i(x, n)xdx = 1. \quad (28)$$

is fulfilled.

The fragmentation functions of quarks and diquarks were changed a little in comparison with Refs. [1, 4] to obtain a better agreement with the existing experimental data, because the old functions [1, 4] correspond to  $\varepsilon = 0$ . We use the quark fragmentation functions in the form

$$G_u^p = G_d^p = a_{\bar{N}}(1-z)^{\lambda+\alpha_R-2\alpha_B}(1+a_1z^2), G_u^{\bar{p}} = G_d^{\bar{p}} = (1-z)G_u^p \quad (29)$$

$$G_u^\Lambda = G_d^\Lambda = \frac{a_{\bar{N}}}{a_{\bar{N}}}(1-z)^{\Delta\alpha}G_u^p, G_u^{\bar{\Lambda}} = (1-z)G_d^\Lambda \quad (30)$$



$$G_d^{\Xi^-} = \frac{a_{\Xi}}{a_{\bar{\Lambda}}}(1-z)^{\Delta\alpha} G_u^p, G_u^{\Xi^-} = G_u^{\Xi} = (1-z)G_d^{\Xi^-} \quad (31)$$

$$G_u^{\Omega} = G_d^{\Omega} = G_u^{\bar{\Omega}} = G_d^{\bar{\Omega}} = \frac{a_{\bar{\Omega}}}{a_{\Xi}}(1-z)^{\Delta\alpha} G_u^{\Xi}, \quad (32)$$

with

$$\Delta\alpha = \alpha_\rho - \alpha_\phi = 1/2, \quad \lambda = 2\alpha' < p_t^2 > = 0.5. \quad (33)$$

Diquark fragmentation functions have more complicate forms. They contain two contributions. The first one corresponds to the central production of a  $B\bar{B}$  pair and can be described by the previous formulas. They have the form:

$$G_{uu}^p = G_{ud}^p = G_{uu}^{\bar{p}} = G_{ud}^{\bar{p}} = a_{\bar{N}}(1-z)^{\lambda - \alpha_R + 4(1 - \alpha_B)}, \quad (34)$$

$$G_{uu}^{\Lambda} = G_{ud}^{\Lambda} = G_{uu}^{\bar{\Lambda}} = G_{ud}^{\bar{\Lambda}} = \frac{a_{\bar{\Lambda}}}{a_{\bar{N}}}(1-z)^{\Delta\alpha} G_{uu}^p, \quad (35)$$

$$G_{uu}^{\Xi^-} = G_{ud}^{\Xi^-} = G_{uu}^{\Xi} = G_{ud}^{\Xi} = \frac{a_{\Xi}}{a_{\bar{\Lambda}}}(1-z)^{\Delta\alpha} G_{uu}^{\Lambda}, \quad (36)$$

$$G_{uu}^{\Omega} = G_{ud}^{\Omega} = G_{uu}^{\bar{\Omega}} = G_{ud}^{\bar{\Omega}} = \frac{a_{\bar{\Omega}}}{a_{\Xi}}(1-z)^{\Delta\alpha} G_{uu}^{\Xi} \quad (37)$$

with the same  $\Delta\alpha$  Eq. (29).

The second contribution is connected with the direct fragmentation of the initial baryon into the secondary one with conservation of the string junction. As discussed above, there exists three different types of such contributions (Figs. 2a-2c). Obviously, in the case of  $\Xi$  production only two possibilities exist with string junction plus either one valence quark and two sea quarks or three sea quarks. In the case of production of a secondary baryon having no common quarks with the incident nucleons only the bare string junction without valence quarks can contribute (Fig. 2c).

All these contributions are determined by Eqs. similar to Eq. (6) with the corresponding fragmentation functions given by

$$G_{uu}^p = G_{ud}^p = a_N \sqrt{z} [v_0 \varepsilon (1-z)^2 + v_q z^{3/2} (1-z) + v_{qq} z^2], \quad (38)$$

$$G_{ud}^{\Lambda} = a_N \sqrt{z} [v_0 \varepsilon (1-z)^2 + v_q z^{3/2} (1-z) + v_{qq} z^2] (1-z)^{\Delta\alpha}, G_{uu}^{\Lambda} = (1-z) G_{ud}^{\Lambda} \quad (39)$$

$$G_{d,SJ}^{\Xi^-} = a_N \sqrt{z} [v_0 \varepsilon (1-z)^2 + v_q z^{3/2} (1-z)] (1-z)^{2\Delta\alpha}, G_{u,SJ}^{\Xi^-} = (1-z) G_{d,SJ}^{\Xi^-}, \quad (40)$$

$$G_{SJ}^{\Omega} = a_N v_0 \varepsilon \sqrt{z} (1-z)^{2+3\Delta\alpha}. \quad (41)$$

The factor  $\sqrt{z}$  is really  $z^{1-\alpha_{SJ}}$  with  $\alpha_{SJ} = 1/2$  (8). As for the factor  $\sqrt{z} z^{3/2}$  of the second term it is just  $2(\alpha_R - \alpha_B)$  [1]. For the third term we have just added an extra factor  $z^{1/2}$ .

The probabilities of transition into the secondary baryon of SJ without valence quarks,  $I_3$ , SJ plus one valence quark,  $I_2$ , and SJ plus a valence diquark,  $I_1$ , were taken from the simplest quark combinatorics [24]. Assuming that the strange quark suppression is the same in all these cases, we obtain for the relative yields of different baryons from SJ fragmentation without valence quarks :

$$I_3 = 4L^3 : 4L^3 : 12L^2S : 3LS^2 : 3LS^2 : S^3 \quad (42)$$

for secondary  $p, n, \Lambda + \Sigma, \Xi^0, \Xi^-$  and  $\Omega$ , respectively.

For  $I_2$  we obtain

$$I_{2u} = 3L^2 : L^2 : 4LS : S^2 : 0 \quad (43)$$

and

$$I_{2d} = L^2 : 3L^2 : 4LS : 0 : S^2 \quad (44)$$

for secondary  $p, n, \Lambda + \Sigma, \Xi^0$  and  $\Xi^-$ .

For  $I_1$  we have

$$I_{1uu} = 2L : 0 : S \quad (45)$$

and

$$I_{1ud} = L : L : S \quad (46)$$

for secondary  $p, n$  and  $\Lambda + \Sigma$ . The ratio  $S/L$  determines the strange suppression factor and  $2L + S = 1$ . In the numerical calculations we used  $S/L = 0.2$ .

In agreement with experimental data we assume that  $\Sigma^+ + \Sigma^- = 0.6\Lambda$  [24] in Eqs. (38)-(40). This is obtained when, say, an  $uus$  state can turn into  $\Sigma^+$  with probability  $3/4$  and into  $\Lambda$  (via  $\Sigma^+(1385) \rightarrow \Lambda\pi^+$  decay) with probability  $1/4$  §. In the case of Eqs. (41) and (42)  $\Sigma^-$  can not be produced and we assume that  $\Sigma^+ = 0.3\Lambda$ .

The values of  $v_0, v_q$  and  $v_{qq}$  are determined directly by the corresponding coefficients of Eqs. (38)-(42), together with the probabilities to fragment a  $qqs$  system into  $\Sigma^+ + \Sigma^-$  and into  $\Lambda$ , given above. For example, we have for incident  $uu$  diquark and secondary proton :

$$v_0 = 4L^3, v_q = 3L^2, v_{qq} = 2L; \quad (47)$$

for incident  $ud$  diquark and secondary proton :

$$v_0 = 4L^3, v_q = 2L^2, v_{qq} = L; \quad (48)$$

for incident  $uu$  diquark and secondary  $\Lambda$  :

$$v_0 = \frac{12}{1.6}SL^2, v_q = \frac{4}{1.6}SL, v_{qq} = \frac{1}{4}S; \quad (49)$$

for incident  $ud$  diquark and secondary  $\Lambda$  :

$$v_0 = \frac{12}{1.6}SL^2, v_q = \frac{4}{1.6}SL, v_{qq} = S; \quad (50)$$

---

§These probabilities are in disagreement with simplest quark statistic rules [28].

for incident  $u$  quark and secondary  $\Xi^-$  :

$$v_0 = 3S^2L, v_q = 0 ; \quad (51)$$

for incident  $d$  quark and secondary  $\Xi^-$  :

$$v_0 = 3S^2L, v_q = S^2 ; \quad (52)$$

and incident SJ and secondary  $\Omega^-$  :

$$v_0 = S^3 . \quad (53)$$

The probability for a process to have  $n$  cutted pomerons was calculated using the quasi-eikonal approximation [1, 27]:

$$w_n = \sigma_n / \sum_{n=1}^{\infty} \sigma_n, \quad \sigma_n = \frac{\sigma_P}{nz} (1 - e^{-z} \sum_{k=0}^{n-1} \frac{z^k}{k!}) , \quad (54)$$

$$z = \frac{2C\gamma}{R^2 + \alpha'\xi} e^{\Delta\xi}, \quad \sigma_P = 8\pi\gamma e^{\Delta\xi}, \quad \xi = \ln(s/1 \text{ GeV}^2) , \quad (55)$$

with parameters

$$\Delta = 0.139, \quad \alpha' = 0.21 \text{ GeV}^{-2}, \quad \gamma_{pp} = 1.77 \text{ GeV}^{-2}, \quad \gamma_{\pi p} = 1.07 \text{ GeV}^{-2}, \\ R_{pp}^2 = 3.18 \text{ GeV}^{-2}, \quad R_{\pi p}^2 = 2.48 \text{ GeV}^{-2}, \quad C_{pp} = 1.5, \quad C_{\pi p} = 1.65 .$$

The model parameters for quark and diquark distributions and their fragmentation are presented in Table 1. They were mainly taken from the description of the data in Refs. [1, 4].

**Table 1**

The values of the parameters used for the calculations in QGSM.

Parameter	value
$a_N$	1.8
$a_{\bar{N}}$	0.18
$a_1$	12
$\alpha_R$	0.5
$\alpha_B$	-0.5

## Figure captions

**Fig. 1.** Cylindrical diagram corresponding to the one-pomeron exchange contribution to elastic  $\bar{p}p$  scattering (a) and its cut which determines the contribution to inelastic  $\bar{p}p$  annihilation cross section (b) (string-junction is indicated by a dashed line). c) the diagram for elastic  $\bar{p}p$ -scattering with an exchange by SJ in the  $t$ -channel and its  $s$ -channel discontinuity d).

**Fig. 2.** Three different possibilities of secondary baryon production in  $pp$  interactions: string junction together with two valence and one sea quark (a), together with one valence and two sea quarks (b), together with three sea quarks (c).

**Fig. 3.** The spectra of secondary protons (a), and antiprotons (b) in  $pp$  collisions at 100 and 175 GeV/c [9] and at 400 GeV/c [15] (c) and (d) and their description by QGSM. Secondary proton (e) and antiproton (f) yields at ISR energies [11] at  $90^\circ$  in c.m.s. and their difference (g) together with QGSM model predictions. In all cases the calculations with  $\epsilon = 0.05$  are shown by solid curves and the variants with  $\epsilon = 0.2$  are shown by dashed curves.

**Fig. 4.** The spectra of secondary antiprotons in  $\pi^-p$  collisions (a) and of protons in  $\pi^+p$  collisions (b) at lab. energies 100 and 175 GeV [9] and its description by QGSM. The differences  $dN/dx$  of  $p - \bar{p}$  yields in  $\frac{1}{2}(\pi^+p + \pi^-p)$  collisions at 158 GeV/c compared to preliminary data from NA49 [10] (c). In all cases the calculations with  $\epsilon = 0.05$  are shown by solid curves and the variants with  $\epsilon = 0.2$  are shown by dashed curves.

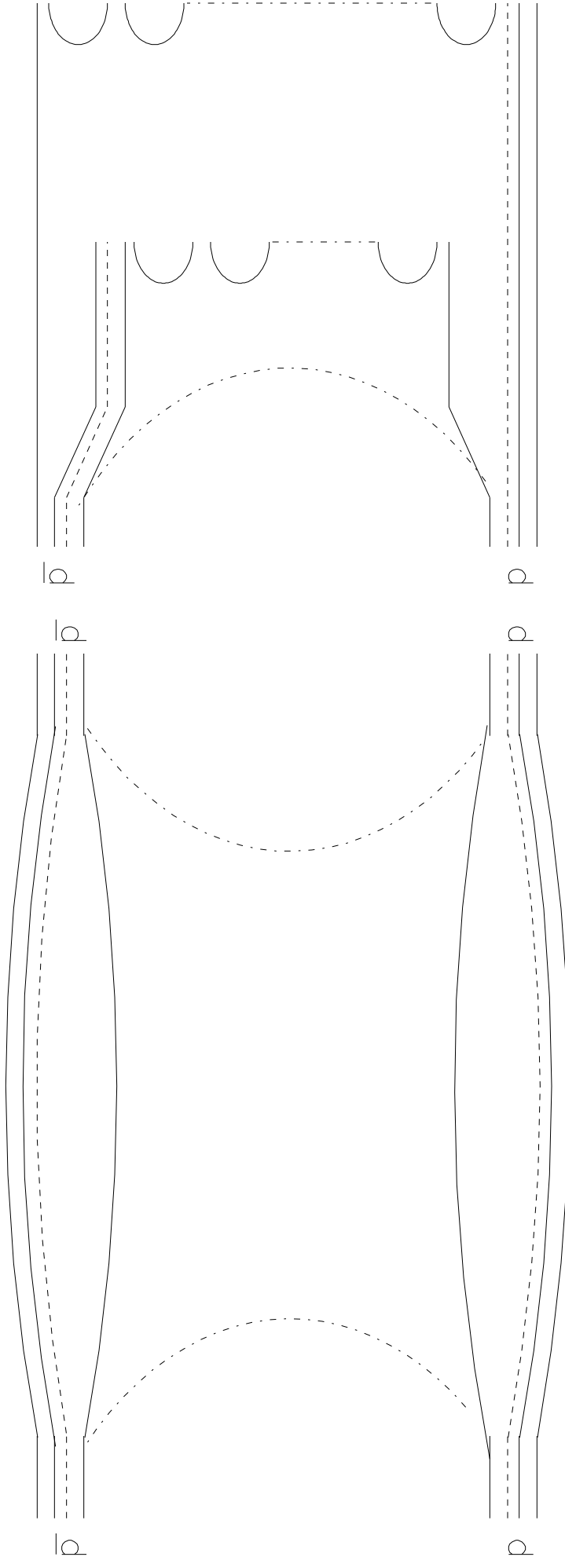
**Fig. 5.** The spectra of secondary  $\Lambda$  (a) and  $\bar{\Lambda}$  (b) in  $pp$  collisions (data are taken from [2]) and its description by QGSM model. The calculations with  $\epsilon = 0.05$  are shown by solid curves and a variant with  $\epsilon = 0.2$  are shown by dashed curves.

**Fig. 6.** The asymmetries of secondary  $\Lambda/\bar{\Lambda}$  (a),  $\Xi^-/\Xi^+$  (b), and  $\Omega/\bar{\Omega}$  (c), in  $\pi^-p$  collisions at 500 GeV/c [12] and its description by QGSM model. In all cases the calculations with  $\epsilon = 0.05$  are shown by solid curves and the variants with  $\epsilon = 0.2$  are shown by dashed curves.

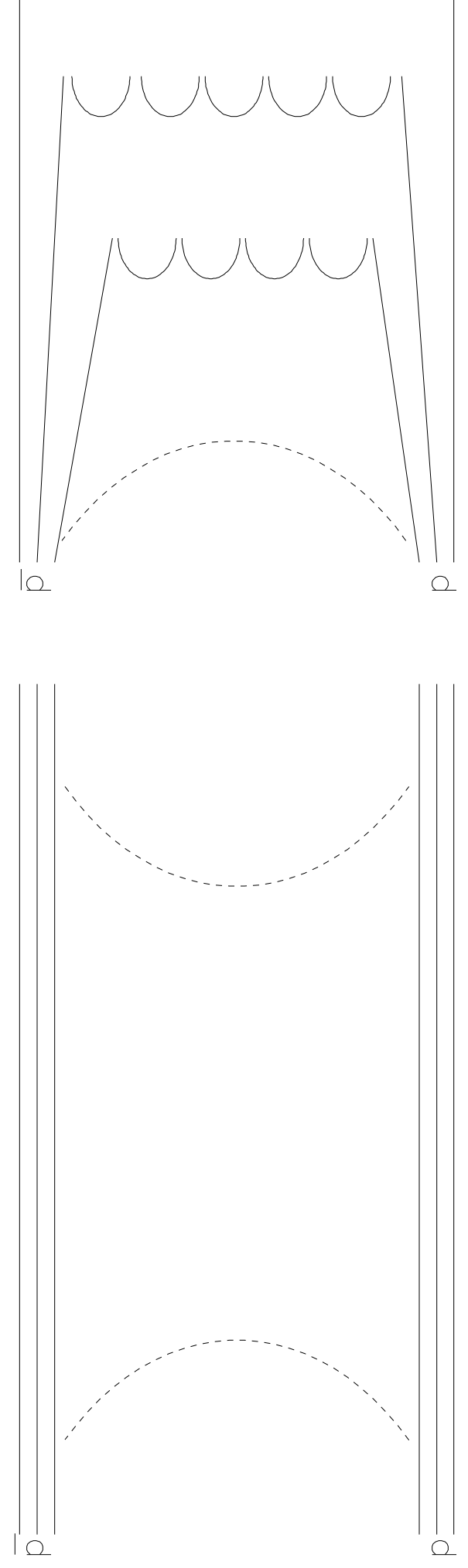
## References

- [1] A. B. Kaidalov and K. A. Ter-Martirosyan, *Yad. Fiz.* 39 (1984) 1545; 40 (1984) 211.  
A. B. Kaidalov and O. I. Piskunova, *Yad. Fiz.* 41 (1985) 1278.
- [2] A. Capella, U. Sukhatme, C. I. Tan and J. Tran Thanh Van, *Phys. Rep.* 236 (1994) 225.  
A. Capella and J. Tran Thanh Van, *Z. Phys. C10* (1981) 249.
- [3] A. B. Kaidalov, K. A. Ter-Martirosyan and Yu. M. Shabelski, *Yad. Fiz.* 43 (1986) 1282.
- [4] Yu. M. Shabelski, *Yad. Fiz.* 44 (1986) 186.
- [5] V. A. Abramovski, V. N. Gribov and O. V. Kancheli, *Yad. Fiz.* 18 (1973) 595.
- [6] A. B. Kaidalov, *Sov. J. Nucl. Phys.* 45 (1987) 902. *Yad. Fiz.* 43 (1986) 1282.
- [7] M. Imachi, S. Otsuki and F. Toyoda, *Prog. Theor. Phys.* 54 (1976) 280; 55 (1976) 551.
- [8] G. C. Rossi and G. Veneziano, *Nucl. Phys.* B123 (1977) 507; L. Montanet, G. C. Rossi and G. Veneziano, *Phys. Rep.* 63 (1980) 149.
- [9] A. E. Brenner et al., *Phys. Rev.* D26 (1982) 1497.
- [10] NA49 collaboration, talk by A. Rybicky at CERN Heavy Ion Forum, 18 October 2000 and private communication by H.G.Fisher.
- [11] M. Banner et al., *Phys. Lett.* B41 (1972) 547; B. Alper et. al. *Nucl. Phys.* B100 (1975) 237.
- [12] E. M. Aitala et al., E769 Coll., hep-ex/0009016.
- [13] C. Adloff et al., H1 Coll. Submitted to the 29th Int. Conf. on High Energy Physics ICHEP98, Vancouver, July 1998.
- [14] B. Z. Kopeliovich and B. G. Zakharov, *Phys. Lett.* B211 (1998) 221.  
E. Gotsman and S. Nusinov, *Phys. Rev.* D22 (1980) 624.
- [15] M. Aguilar-Benitez et al., LEBC-EHS Coll. *Z.Phys.* 50 (1991) 405.
- [16] J. W. Chapman et al., *Phys. Lett.* B47 (1973) 465.
- [17] H. Boggild et al., *Nucl. Phys.* B27 (1971) 285.
- [18] A. Sheng et al., *Phys. Rev.* D11 (1975) 1733.

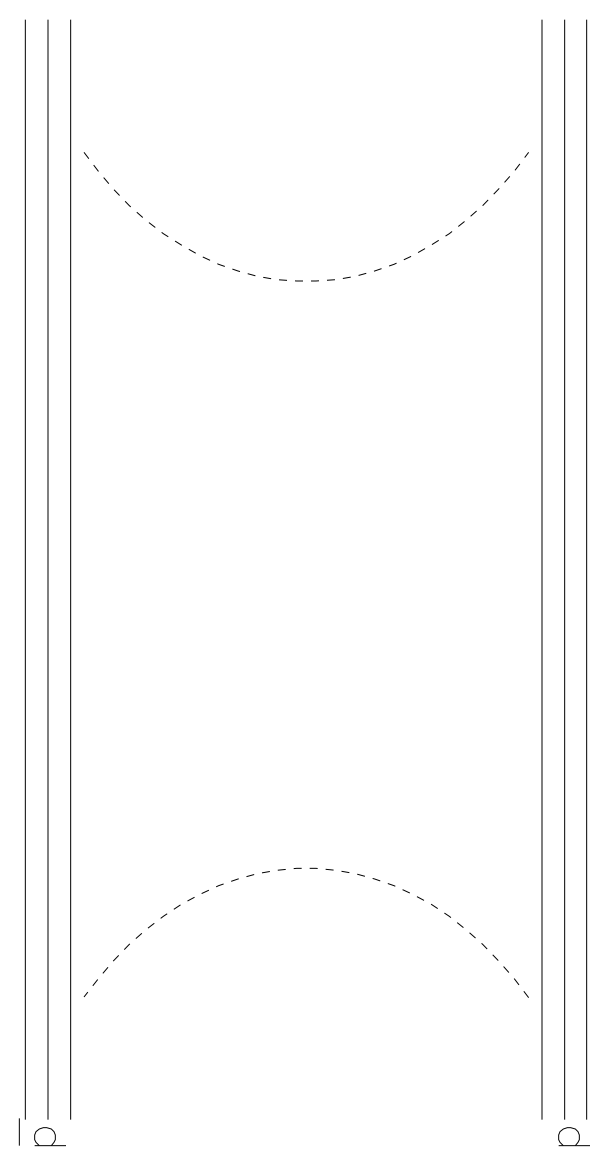
- [19] H. Kichimi et al., Phys. Rev. D20 (79) 37.
- [20] E. M. Aitala et al., E769 Coll., hep-ex/0008029.
- [21] B. Kopeliovich and B. Povh, Phys. Lett. B446 (1999) 321.
- [22] A. Capella and B. Z. Kopeliovich, Phys. Lett. B381 (1996) 325.
- [23] A. Capella, E. G. Ferreira and C. Salgado, Phys. Lett. B459 (1999) 27.
- [24] A. Capella and C.-A. Salgado, Phys. Rev. C60 (1999) 054906.
- [25] D. Kharzeev, Phys. Lett. B378 (1996) 238.
- [26] S. E. Vance and M. Gyulassy, Phys. Rev. Lett. 83 (1999) 1735.
- [27] K. A. Ter-Martirosyan, Phys. Lett. 44B (1973) 377.
- [28] V. V. Anisovich, M. N. Kobrinsky, J. Nyiri and Yu. M. Shabelski, Soviet Physics - Usp. Fiz. Nauk 144 (1984)553; Quark Model and High Energy Collisions. World Scientific, Singapore, 1985.



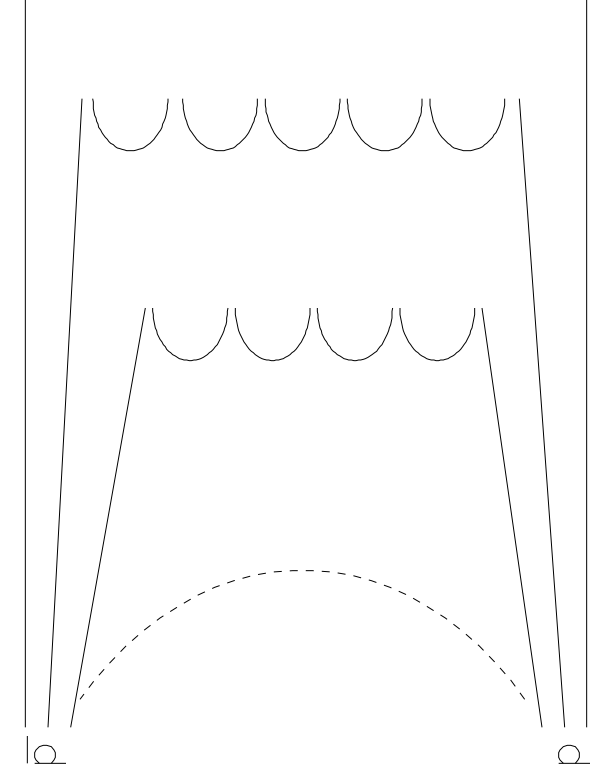
a)



b)



c)



d)

Fig. 1



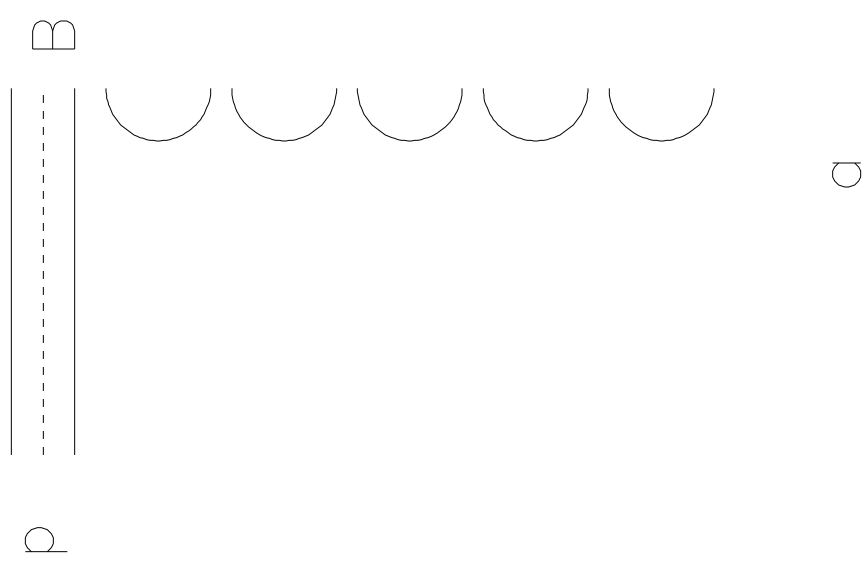
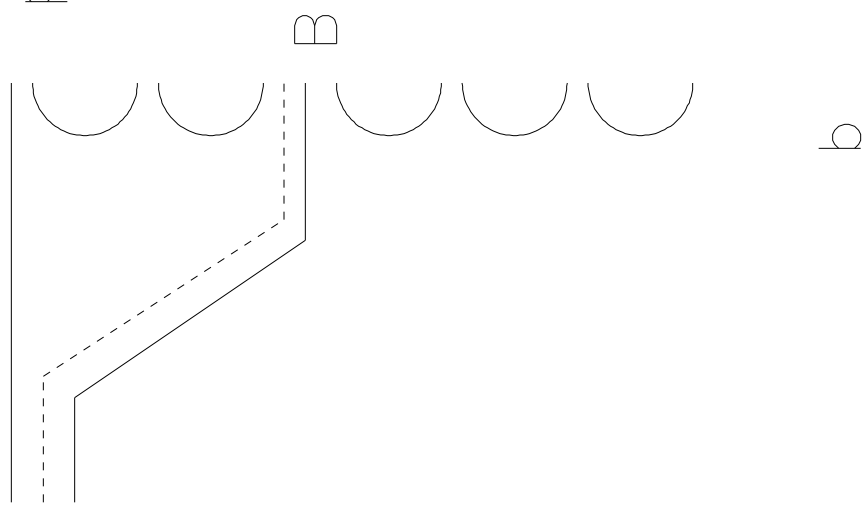
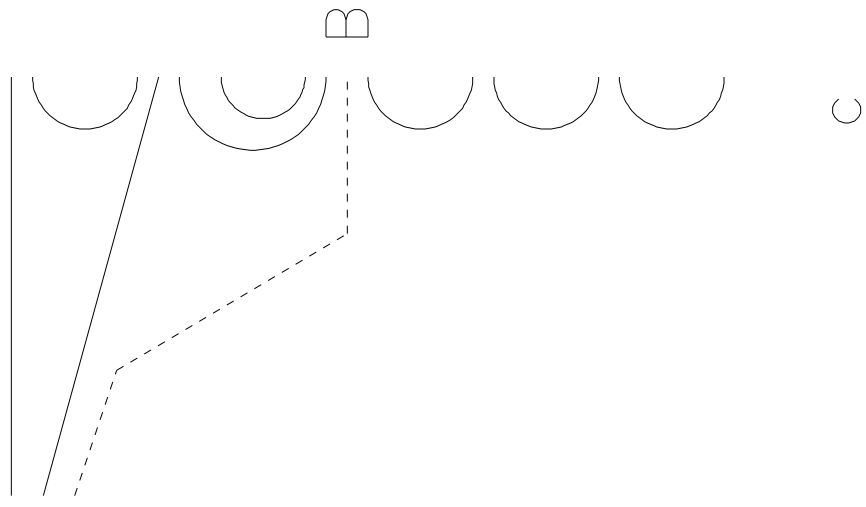


Fig. 2

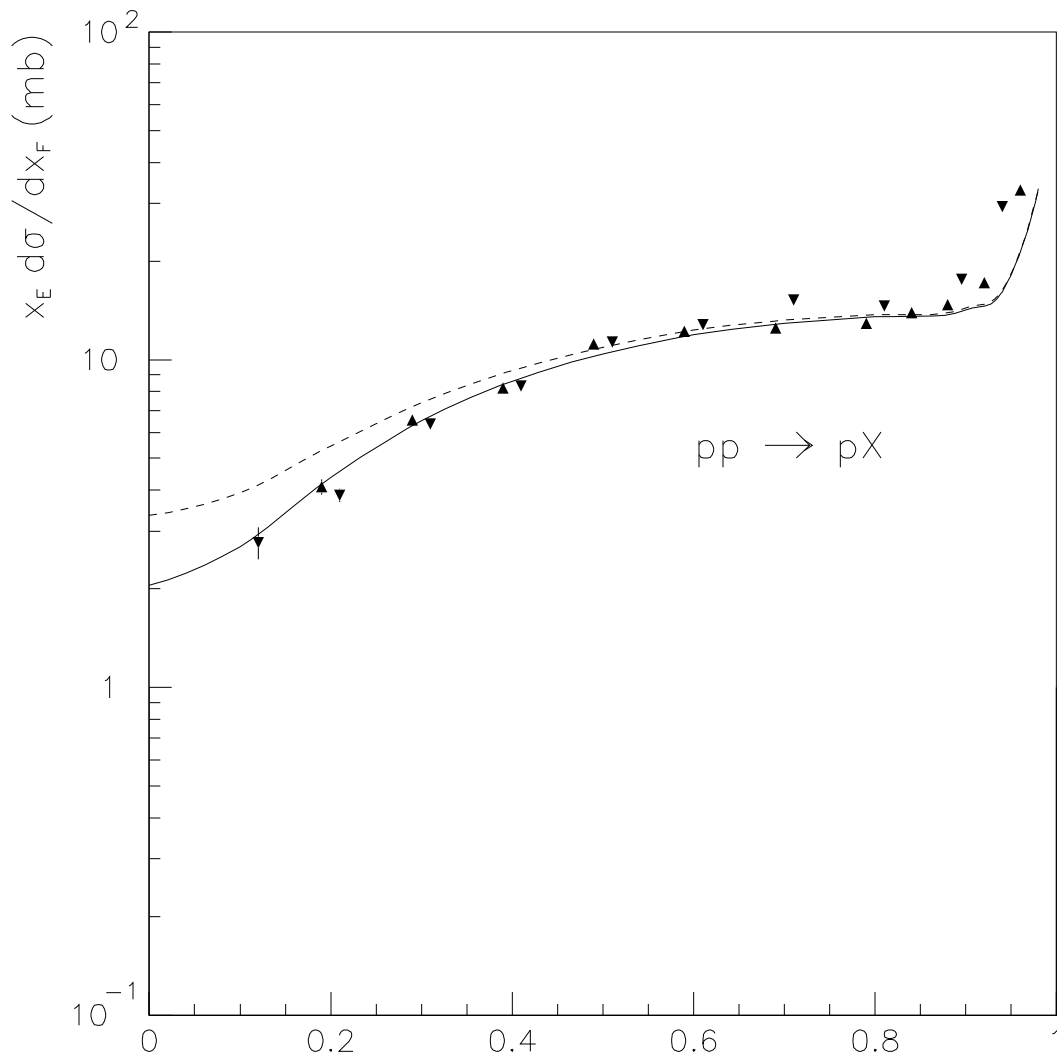


Fig. 3a

$x_F$

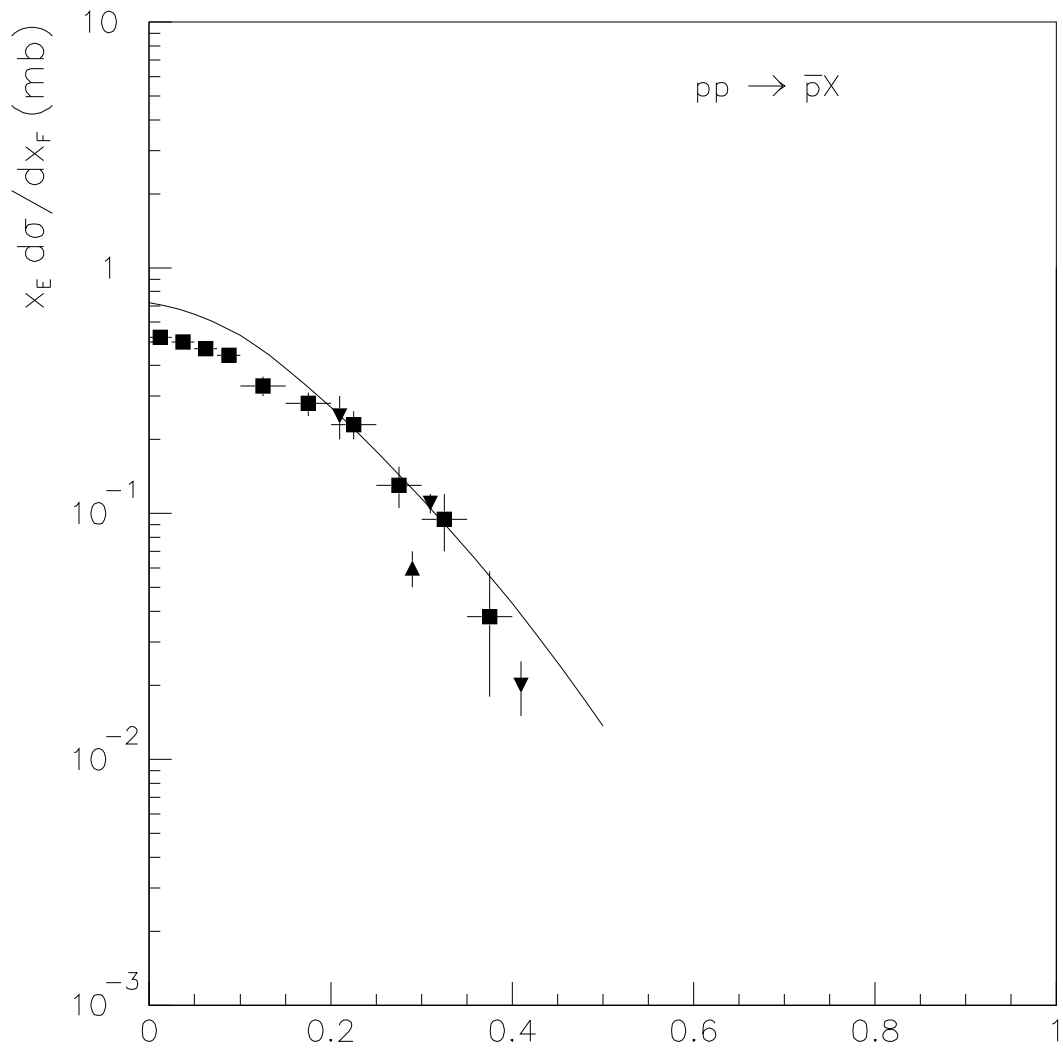


Fig. 3b

$x_F$

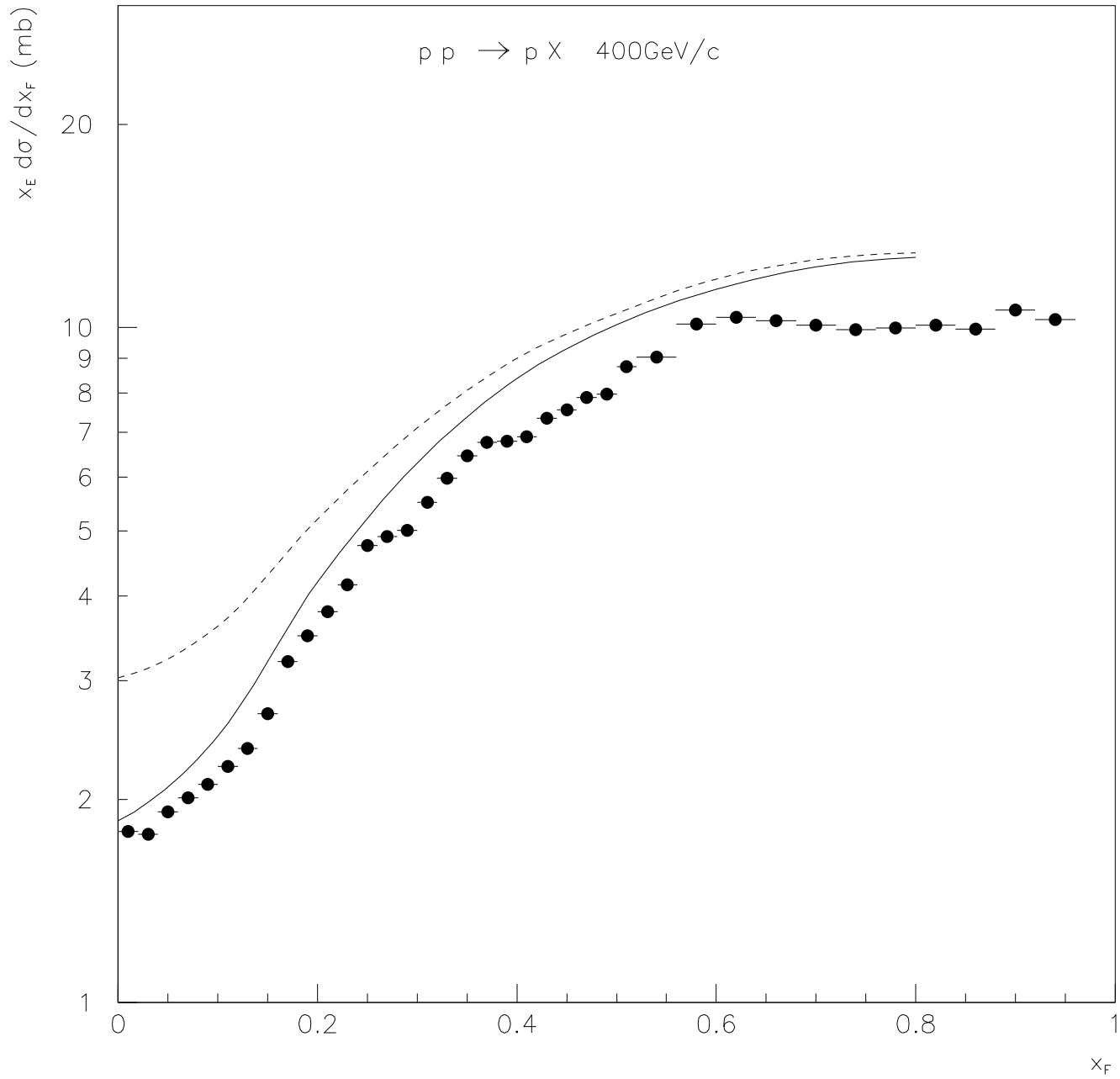


Fig. 3c

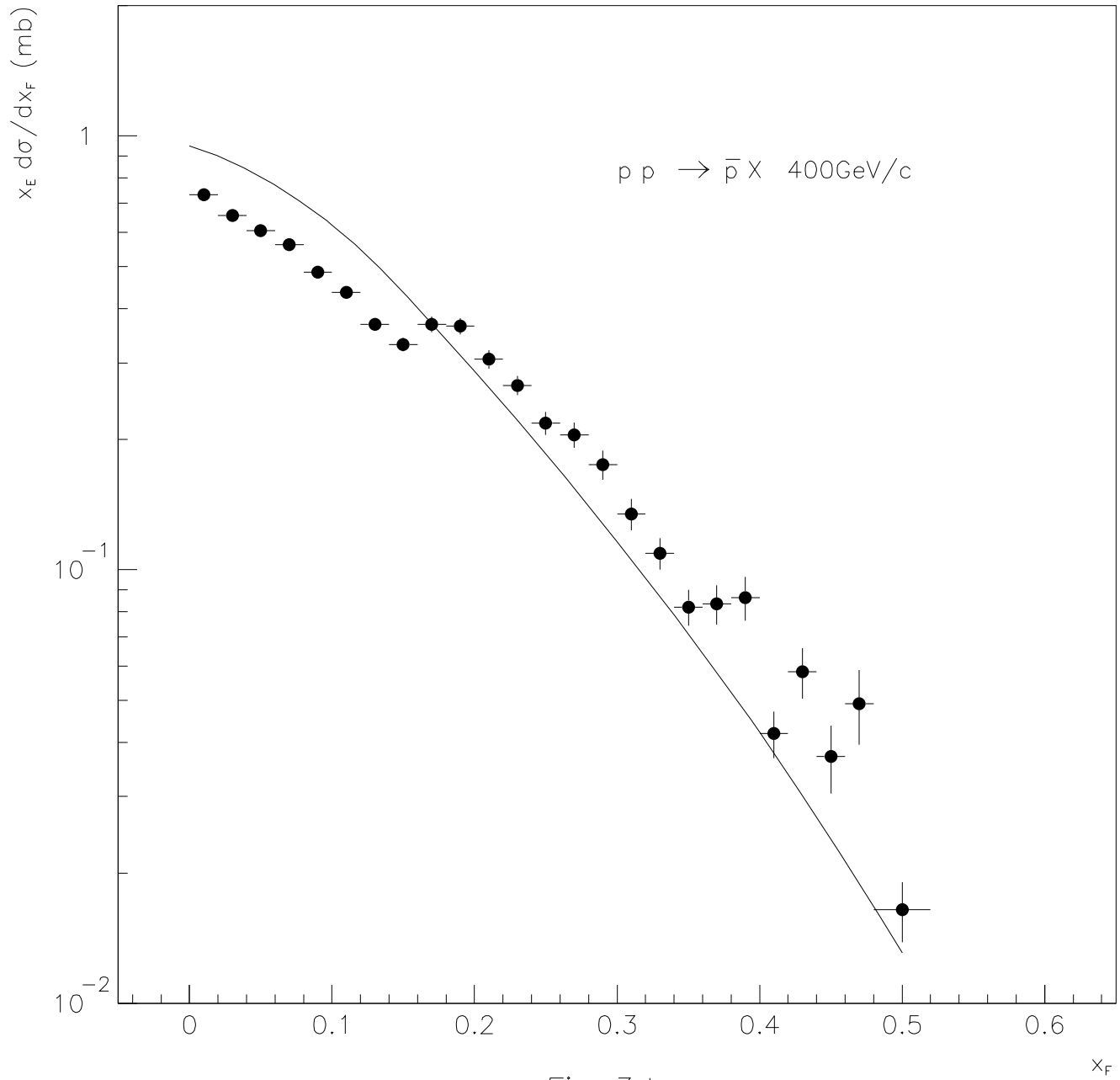


Fig. 3d

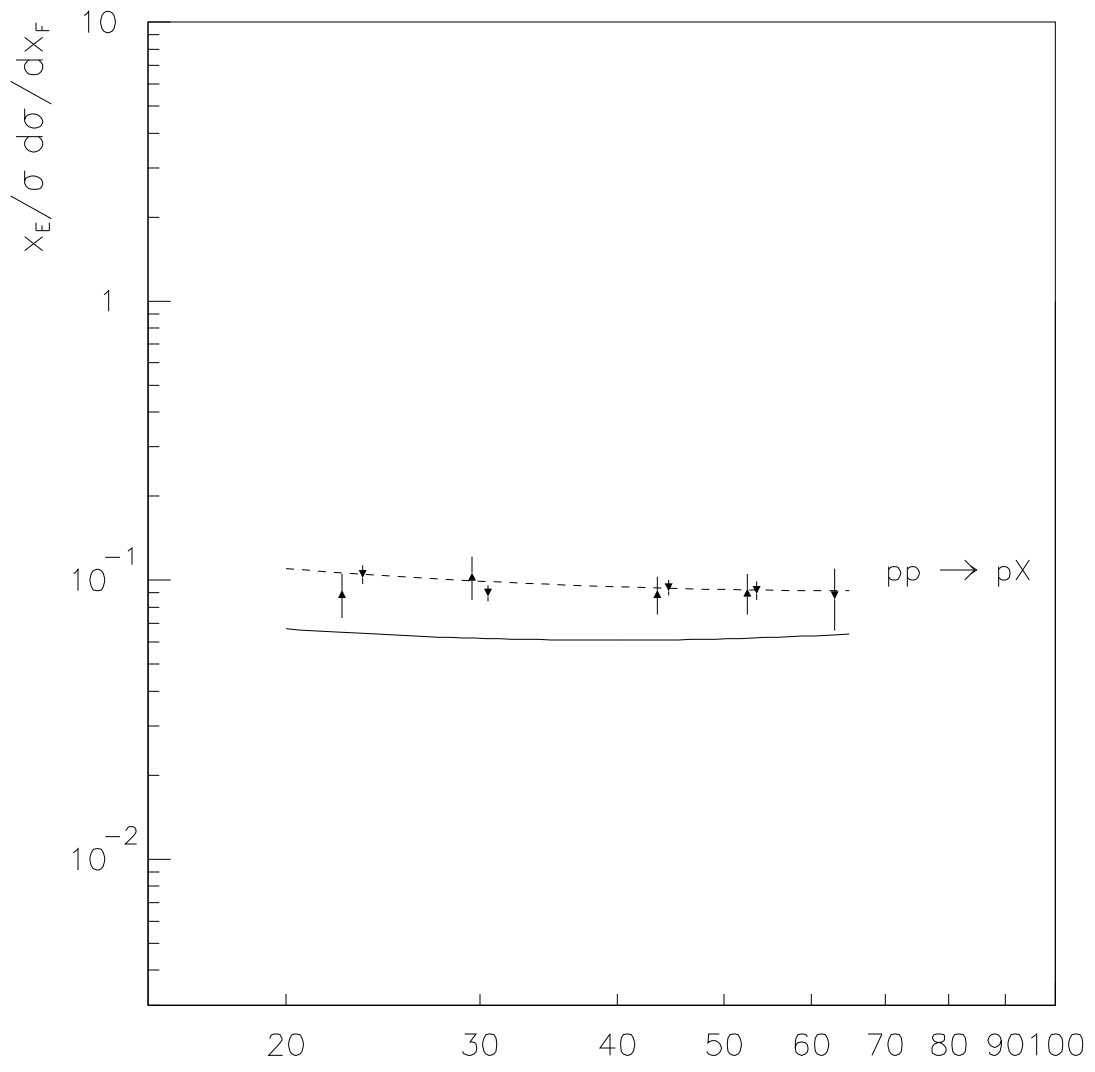


Fig. 3e  $\sqrt{s}$  (GeV)

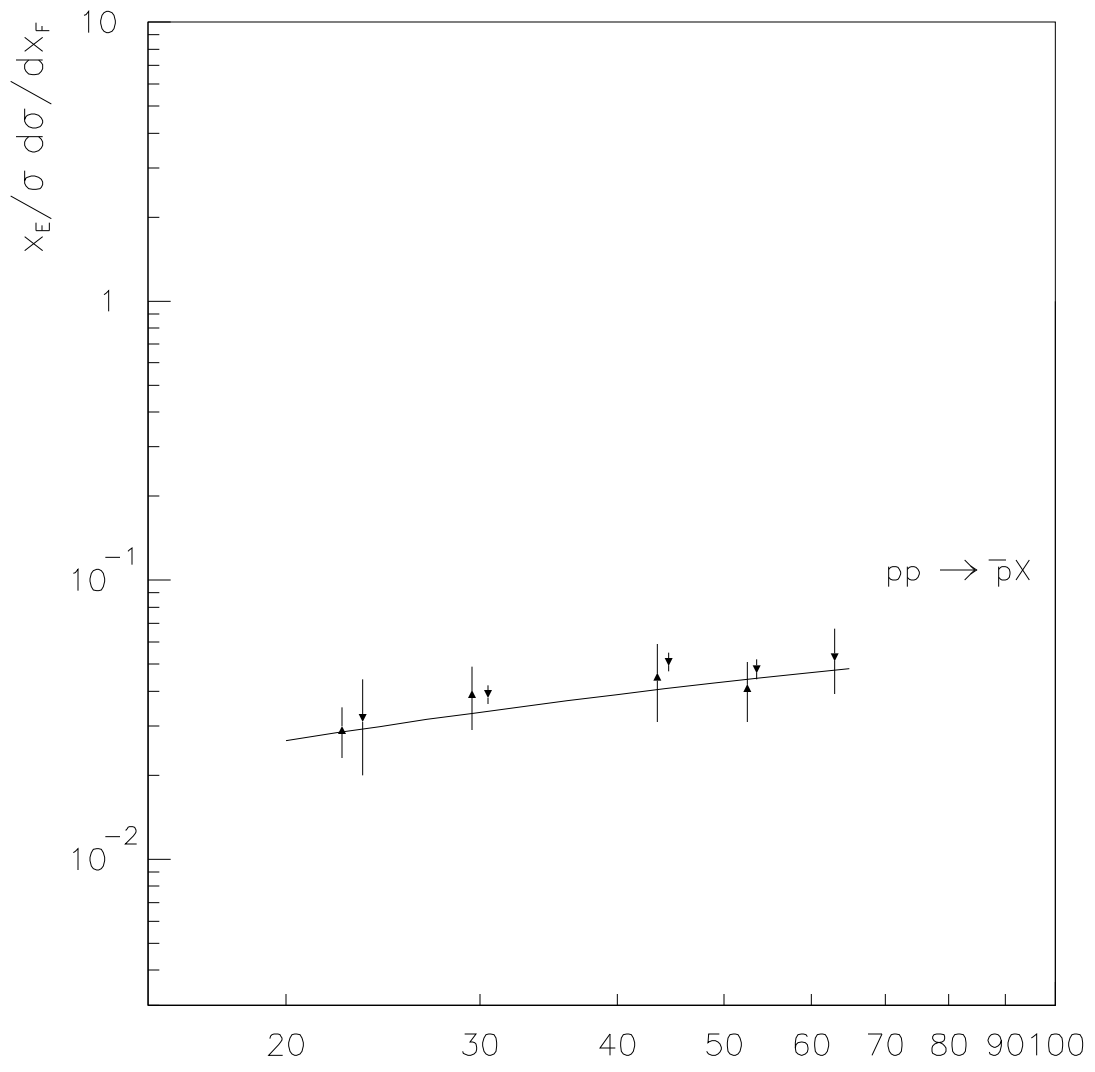


Fig. 3f  $\sqrt{s}$  (GeV)

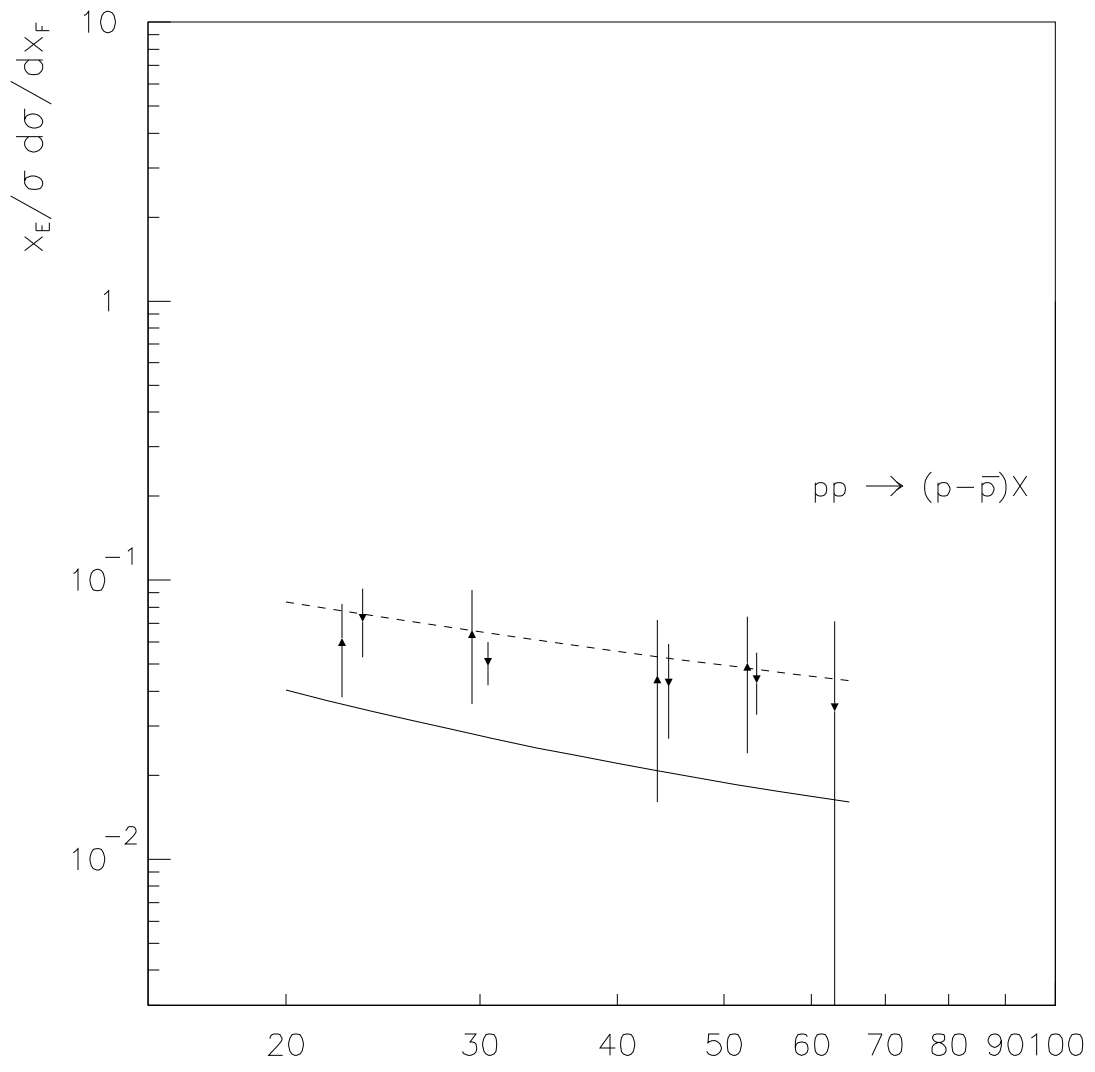


Fig. 3g  $\sqrt{s}$  (GeV)



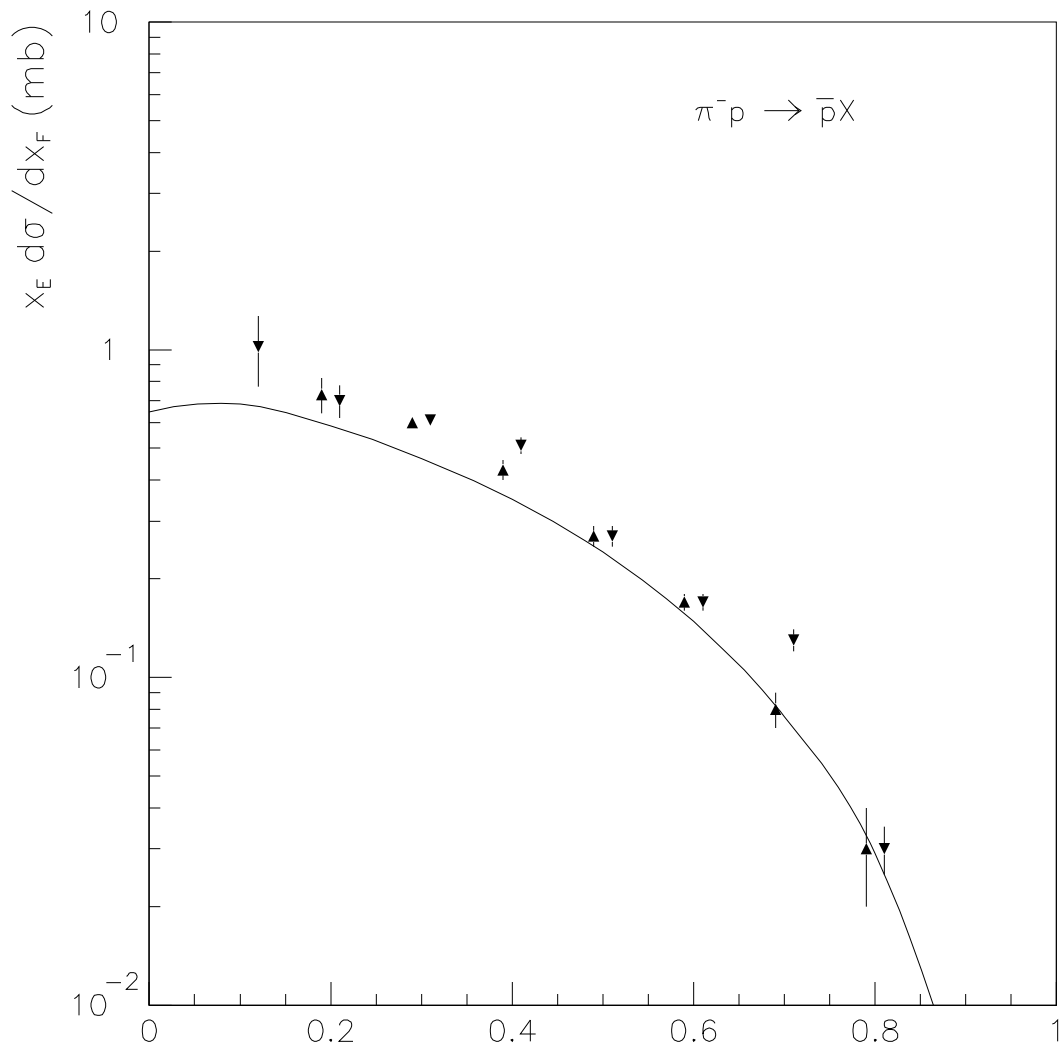


Fig. 4a

$x_F$

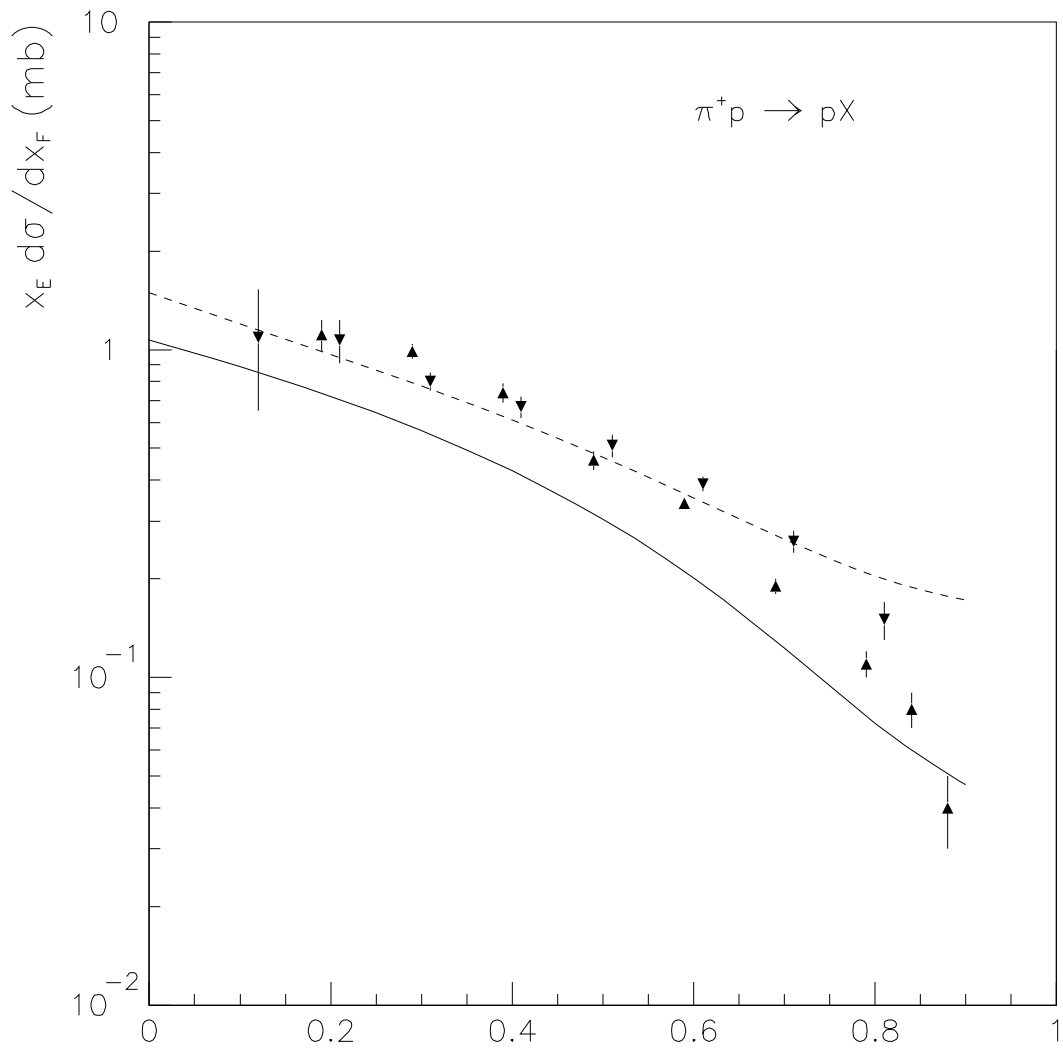


Fig. 4b

$x_F$

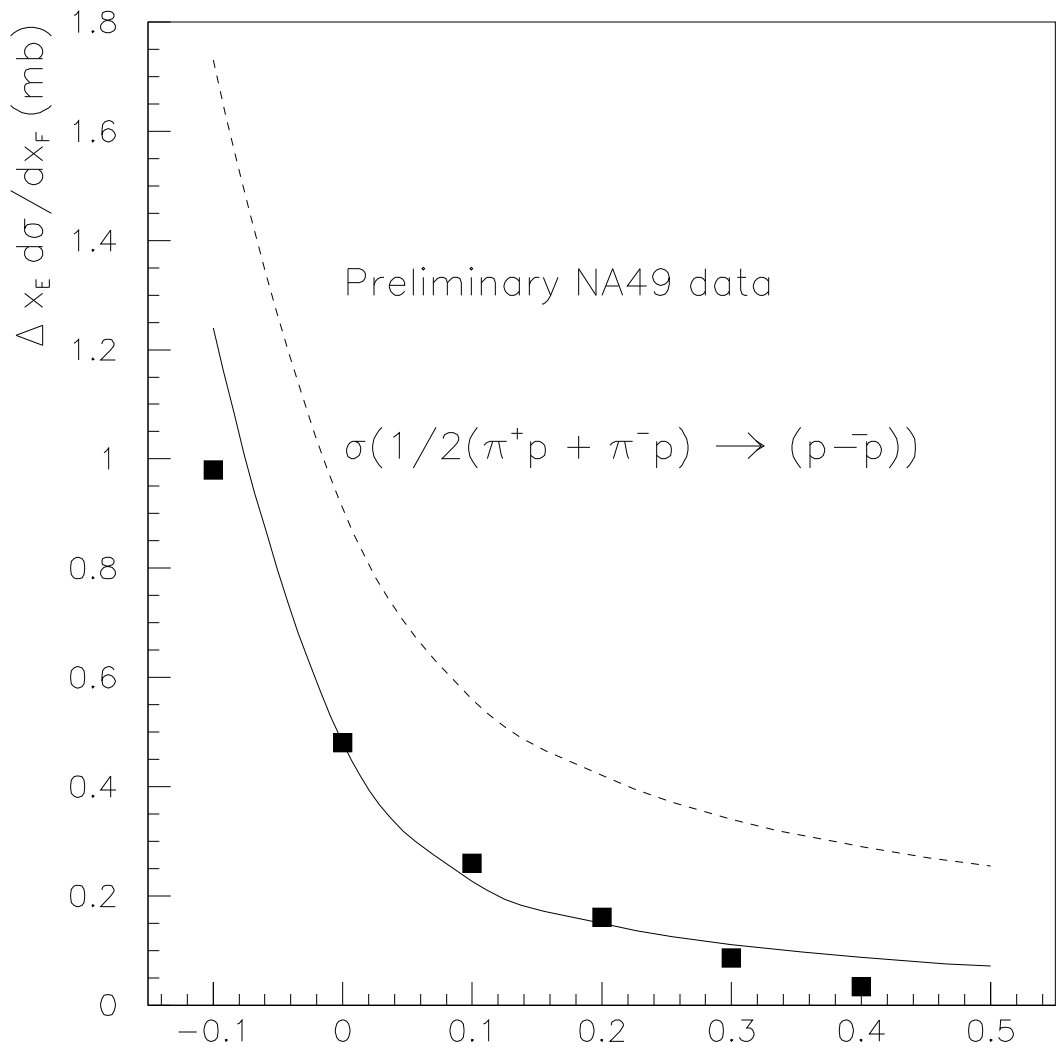


Fig. 4c

$x_F$

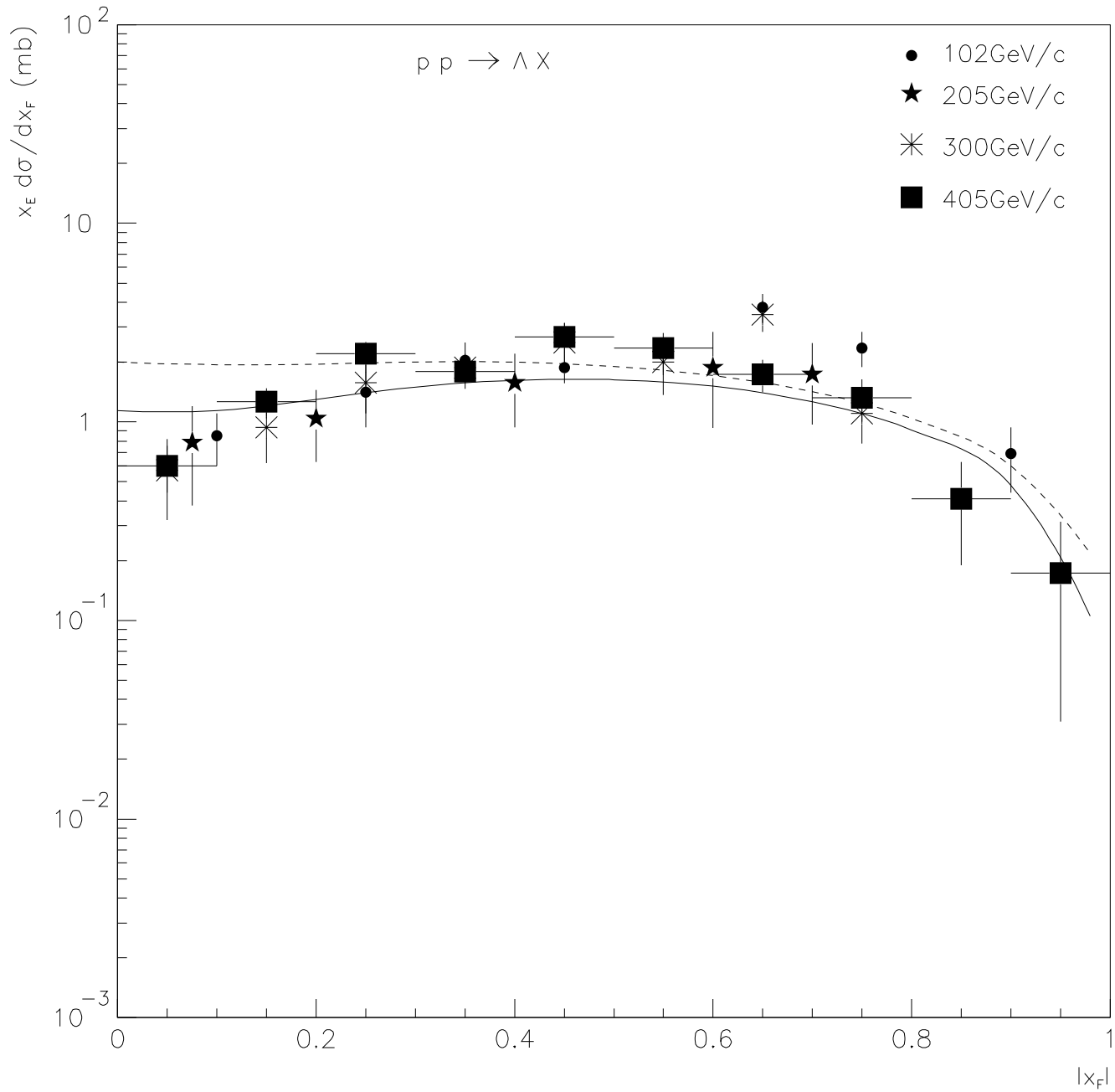


Fig. 5a

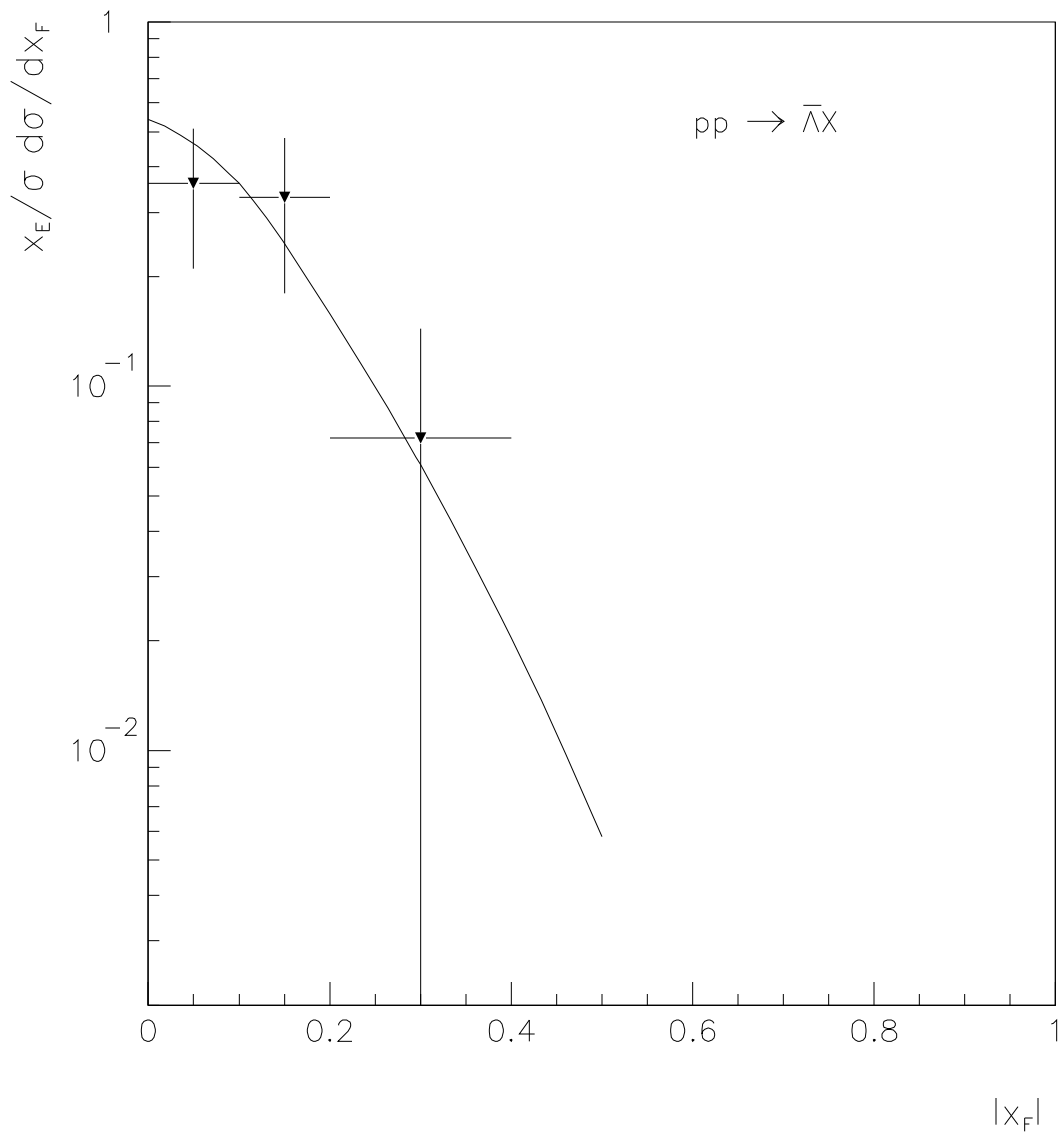


Fig. 5b

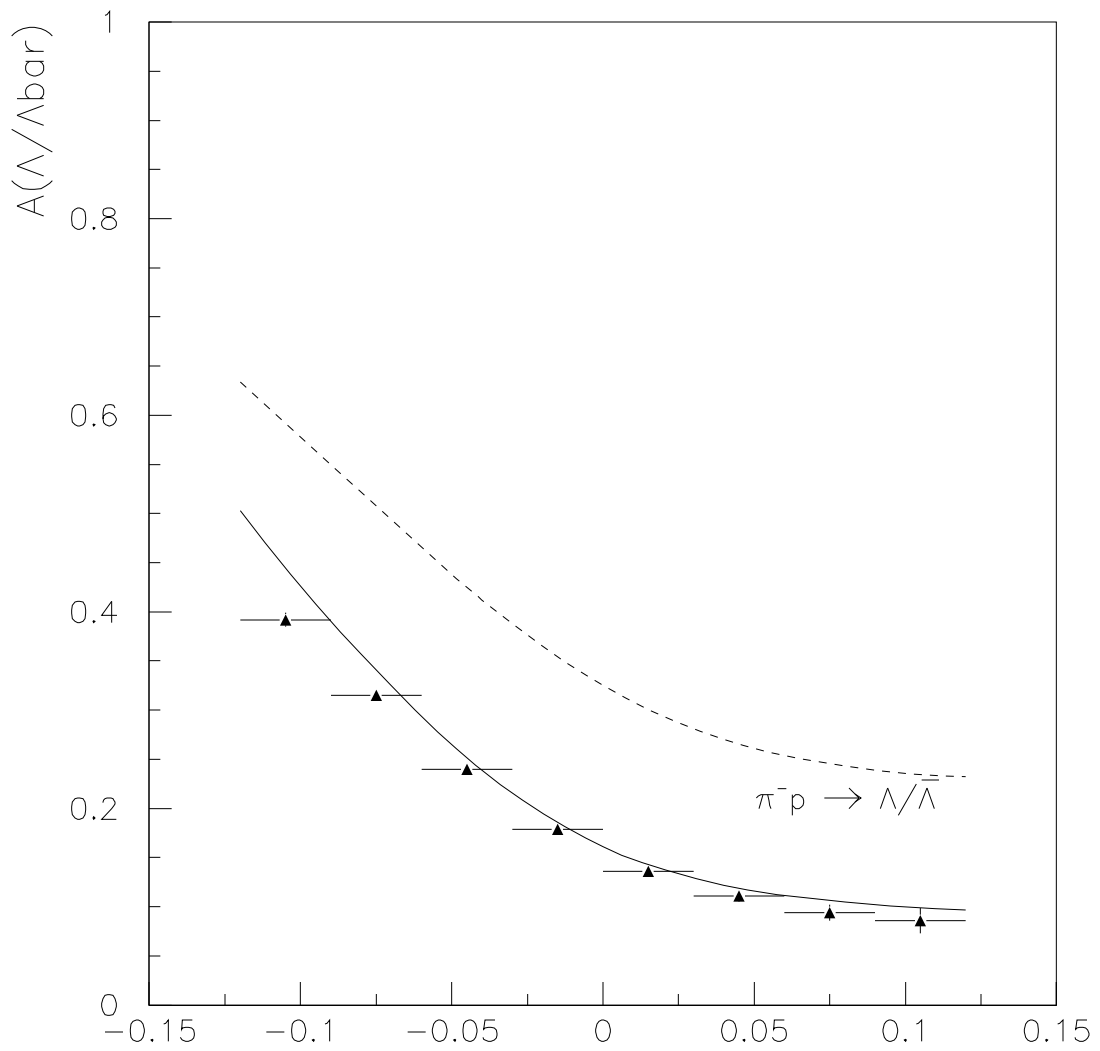


Fig. 6a

$X_F$

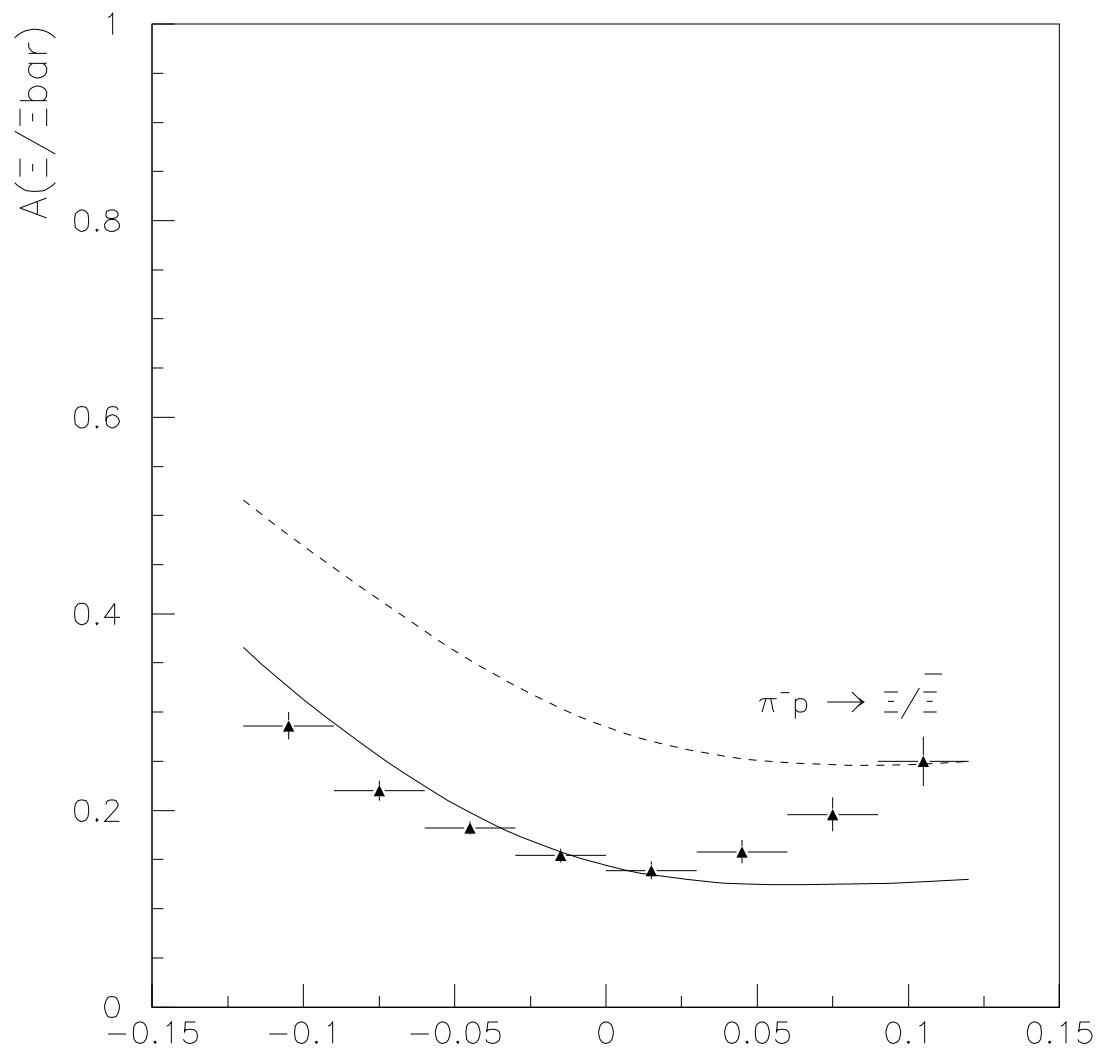


Fig. 6b

$X_F$

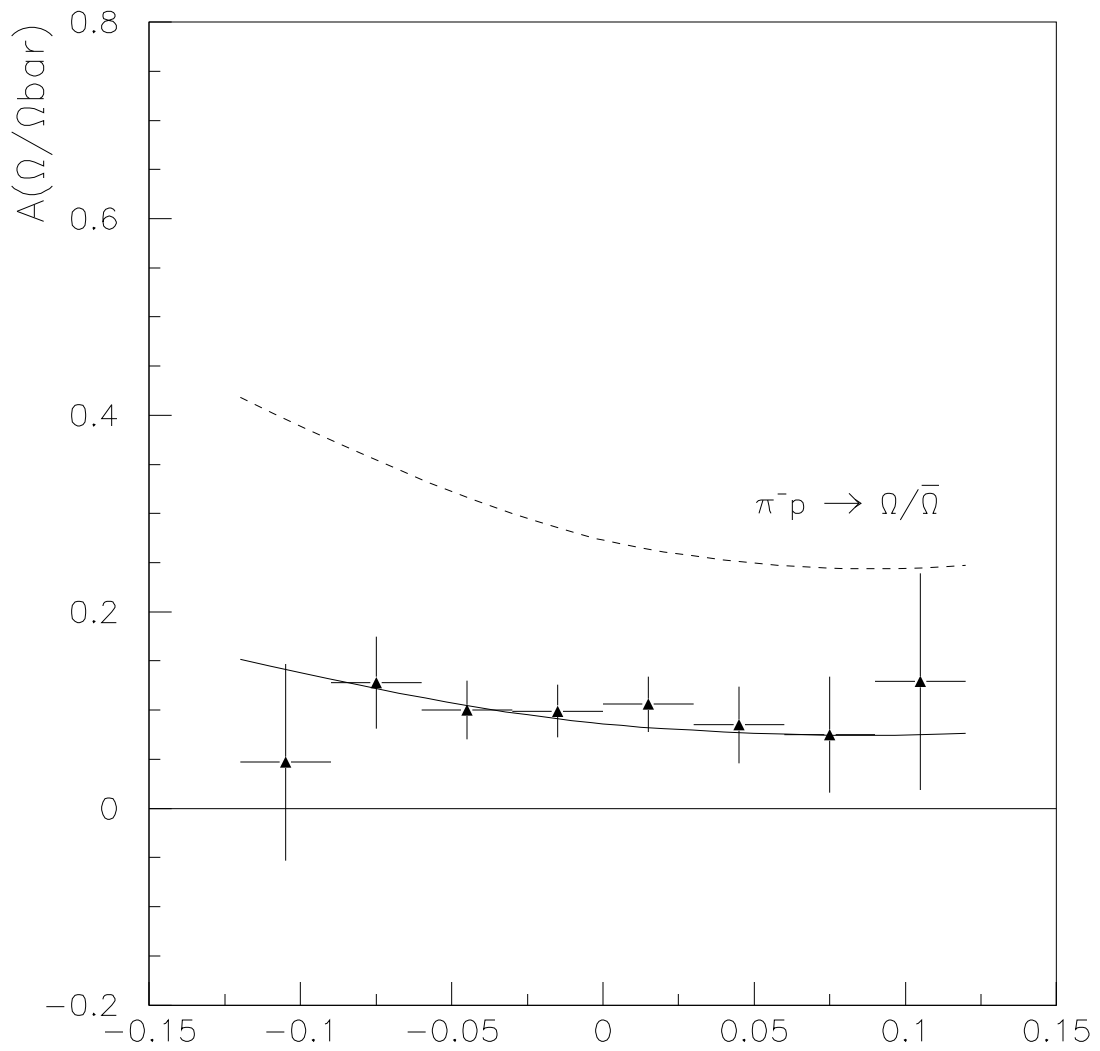


Fig. 6c

$X_F$